REVIEW—Multiferroics Special Section

This section of Journal of Materials Research is reserved for papers that are reviews of literature in a given area.

Electrical characterization of magnetoelectrical materials

J.F. Scott[a)]
Centre for Ferroics, Earth Sciences Department, University of Cambridge, Cambridge CB2 3EQ, United Kingdom

(Received 9 November 2006; accepted 19 January 2007)

A brief review is given of electrical properties of magnetoelectric, multiferroic materials, with emphasis on magnetocapacitance effects, nanostructures, integration into real random access memories, and critical phenomena, including defect dynamics near phase transitions.

I. INTRODUCTION

Materials that are simultaneously ferroelectric and ferromagnetic were originally termed "magnetoelectric" but more recently have been called "multiferroic." In addition to being of considerable academic interest because of the ways in which electric polarization P can couple with magnetization M, they are also of potential interest for use in engineering devices as random-access memory (RAM) elements; in this application, they can be read magnetically (nondestructive readout with no reset operation required), and they can be erased and rewritten electrically (faster and less power-consuming than magnetic rewrite). They also have potential device application as weak-magnetic-field sensors; these would be similar in performance to superconducting quantum interference devices but would be operational at ambient temperatures; hence, much cheaper.

The search for materials that would be good magnetoelectric materials began in earnest in the late 1950s in Leningrad in the group of Prof. Smolenskii at the Ioffe Institute.[1] The materials studied included $BiFeO_3$ and other perovskite oxides, generally doped (most recently with Mn) to make them better insulators and less semiconducting. Transition metal oxides are rarely good insulators because of oxygen vacancies and/or multivalent metal ions.

II. PITFALLS AND ARTIFACTS

Electrical measurements of ferroelectrics in the earlier years (1920–1980) were generally made on bulk insulators. Under these conditions, the measurements of hysteresis were usually performed with a Sawyer–Tower circuit, which actually measured the switched charge Q, typically at a frequency (f) of 50 or 60 Hz. This is important; nature does not provide us with a simple way of directly measuring polarization P. For an ideal insulator, the charge switched is determined by the displacement current dD/dt in the system, where for most ferroelectrics the displacement vector D from Maxwell's equations is nearly the same as polarization P. In a parallel plate capacitor, the switched charge when polarization is reversed in a ferroelectric is $Q = 2AP_r$, where A is the area of the electrode and P_r is the remanent polarization. If the material is not a perfect insulator, in addition to the displacement current dP/dt there will be a real conduction with current $j = \sigma EA$ where σ is the electrical conductivity, and hence an additional injected charge $Q = \sigma EAt$, where t is the time of the applied positive field ($1/2f$). This injected charge may be very large, particularly in magnetoelectric materials, because they are rarely good insulators. Therefore, many published measurements of what appears to be hysteresis in magnetoelectric materials are often complete artifacts, resulting from charge injection. The measured "hysteresis" loops are usually rather rounded, often cigar-shaped, and arise from a combination of injected charge and electrical loss; the hysteresis curves are not saturated (linear and nearly flat at large fields E) and may even be nonmonatonic with increasing field or voltage.

A related problem is that of curves that are too flat. As discussed in elementary textbooks (e.g., Jaffe et al.[2]), hysteresis measurements are often limited by the saturation of the amplifiers in the detection equipment. This gives a very square hysteresis curve that is absolutely flat. However, because the slope of P versus E for small E must give the dielectric constant, having a truly flat hysteresis curve would imply an unphysical dielectric constant e of zero.

[a)]Address all correspondence to this author.
e-mail: jsco99@esc.cam.ac.uk
This paper is based on tutorial notes used at the MRS meeting in Boston, November 2006.
DOI: 10.1557/JMR.2007.0260

All of these points are well known for ordinary ferroelectrics and have been reviewed recently,[1] but they should be reemphasized here because they are exaggerated in thin films compared with bulk, and in magnetoelectric materials compared with more ordinary ferroelectrics, in each case because the conductivity is typically higher.[3,4]

III. BASIC PHYSICS

There was a brief period in the 1920s, shortly after ferroelectricity was first discovered (1920), during which Perrier and Staring[5,6] claimed to have discovered magnetoelectricity in materials such as nickel in which the effect cannot exist. This put magnetoelectricity under a black cloud, similar to that recently experienced in the scientific community with cold fusion or polywater. Very few researchers would dare working in this area. That changed in the late 1950s in Moscow, where physicists understood magnetic symmetry very well. They recognized that linear magnetoelectricity, with a Hamiltonian or free energy of form

$$G(P, M, T) = \alpha_{ij}\, P_i\, M_j \quad , \qquad (1)$$

is quite realistic, albeit not time-reversal-invariant. Magnetic materials need not have time-reversal-invariant Hamiltonians, although a 50%–50% distribution of domains will do so in a global sense. Similarly, piezomagnetism, which is a linear coupling of magnetization with strain S is perfectly allowed and is analogous to piezoelectricity.

A. The linear magnetoelectric effect

A specific prediction of a linear magnetoelectric effect was made by Dzyaloshinskii[7] in 1957 in the antiferromagnet Cr_2O_3 and confirmed soon after by Astrov.[8] A similar prediction of piezomagnetism (in MnF_2) was soon confirmed by Borovik-Romanov.[9]

B. The quadratic magnetoelectric effect

There are "higher-order" couplings between polarization and magnetization. In particular the quadratic term

$$G(P, M, T) = \beta_{ijk}\, P_i\, M_j\, M_k \quad , \qquad (2a)$$

is much larger than the linear term in practically all cases, and it can be large when the linear term is exactly zero (forbidden by symmetry). This term was first measured in detail by Hou and Bloembergen[10] at Harvard. It is also important to note that this term can be large well above the Nèel temperature (T_N) where the expectation value $\langle M_i \rangle = 0$ and hence the linear magnetoelectric effect vanishes. This was first shown by Scott[11,12] in $BaMnF_4$ and occurs in any magnetic system in which in-plane ordering occurs, a two-dimensional (2D) ordering; this is not uncommon and results in a term

$$G(P, M, T) = \beta_{ijj}\, P_i \langle M_j\, M_j \rangle \quad , \qquad (2b)$$

which varies with temperature as the magnetic energy (Scott[11] and Glass et al.[12]) and typically vanishes only for $T > 3T_N$. In each case, these interactions produce dielectric anomalies; typically, the linear coupling in Eq. (1) produces an anomaly at T_N along the polar axis (Fig. 1), whereas the quadratic term in Eq. (2b) gives an anomaly (Fig. 2) at T[2D], which is the temperature at which 2D in-plane spin ordering occurs (where T[2D] is typically $\sim 3T_N$).

Ferroelectricity can cause ferromagnetism! In 1977, Fox and Scott showed[15] that in systems of low symmetry ferroelectricity can cause weak ferromagnetism in materials that otherwise would be simple antiferromagnetics. This occurs via the Dzyaloshinskii–Moriya anisotropic exchange and can take place in $BaMnF_4$ (magnetic symmetry 2′) but not in $BaCoF_4$ (magnetic symmetry 2). The

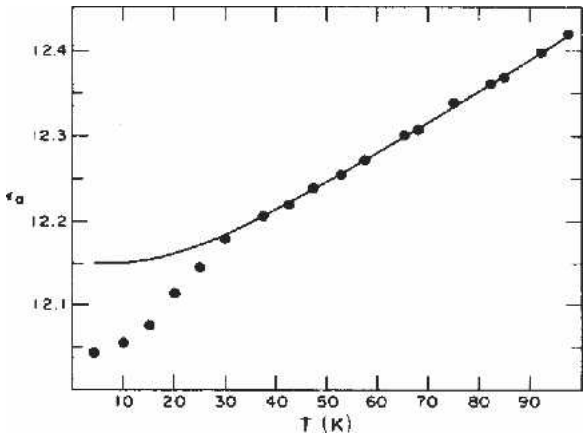

FIG. 1. Dielectric anomaly at T_N along the polar a axis in $BaMnF_4$; this anomaly is proportional to the square of the magnetization $M(T)$. The solid curve is a careful fit to a theory giving the dielectric constant in the absence of magnetic ordering.[13,14]

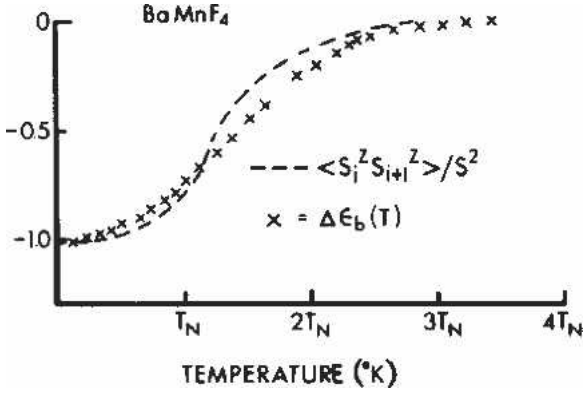

FIG. 2. Dielectric anomaly along the b axis in $BaMnF_4$ near the in-plane two-dimensional ordering temperature T_{2D}; this anomaly is proportional to the magnetic energy $\langle S_i\, S_j \rangle$.[11,12]

physical mechanism involved is that the ferroelectric displacements alter the Mn–ion exchange integral.

C. Magnetodielectric effects (magnetocapacitance)

There are at least three different kinds of magnetodielectric anomaly. The two simplest intrinsic kinds are in the first-case proportional to the square of the sublattice magnetization $<M^2(T)>$ and, in the second case, proportional to the nearest-neighbor magnetic energy $<S_j\ S_{j+1}>$. These two cases have very specific temperature dependencies and are rather frequency-independent. Note that the latter case can persist well above the magnetic ordering temperature T_N in systems with planar (2D) spin-ordering, whereas the former case vanishes exactly at T_N. These intrinsic dielectric anomalies are usually negative (smaller dielectric constant) and on the order of 0.1%–3.0%. The third case is extrinsic and arises in any magnetoresistive material with space charge. Such Maxwell–Wagner effects can occur at grain boundaries in ceramics or at electrode interfaces in single crystals. The temperature dependence is frequency-dependent and looks like the dielectric anomaly in a relaxor. It can be of either sign but is usually positive and very large; it can exceed 1000%. In any magnetoelectric material, there will be a change in the dielectric constant at the magnetic ordering temperature (which here is denoted as T_N for Nèel temperature; it is used even in the case of ferromagnets, as a symbol for any magnetic ordering, in order not to confuse the ferromagnetic Curie temperature T_C with the ferroelectric T_C).

Unfortunately, such magnetocapacitance effects can be complete artifacts. As shown by Catalan,[16] any magnetoresistive material that also has a Maxwell–Wagner space charge will have a magnetodielectric effect. These can be very large (Egami[17] has measured >1000% change in ϵ). It is my opinion that such extrinsic artifacts probably explain the anomalies reported by Loidl's group[18–21] in both chromium cadmium spinel and mercury cadmium spinel (a 450% effect). This would reconcile the paradox observed by Fennie and Rabe[22] at Rutgers, that the samples (grown without Cl-flux) have no anomalies. It would seem that the space charge caused by the Cl-ions might be the culprit here. In my opinion, these spinels are probably cubic, as shown by Fennie and Rabe[22] and not even ferroelectric, let alone magnetoelectric. Catalan and Scott[23] have made a similar analysis for magnetodielectric anomalies in $(NbSe_4)_3I$ (Fig. 3).

D. Domains

The presence of magnetism and ferroelectricity obviously complicates domain structures. These are particularly interesting for nano-sized devices. Because any memory element is likely to be on the order of 400 nm × 400 nm × 100 nm or smaller, we can begin by considering domains in such submicron specimens.

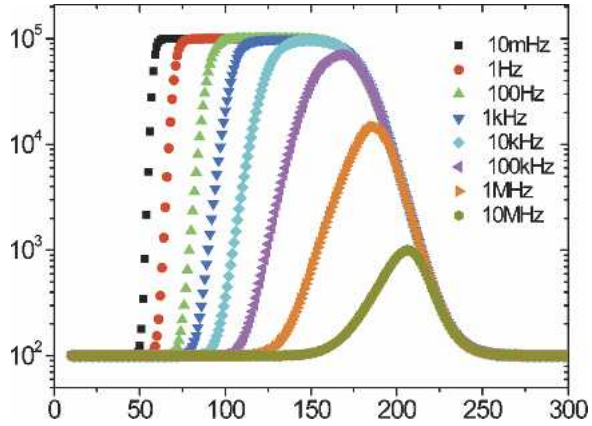

FIG. 3. The calculated real part of the dielectric constant in a Maxwell–Wagner equivalent circuit with parameters as described in the main text (from Catalan and Scott[23]). This calculation does not incorporate the contact-related additional dielectric enhancement above ~200–250 K. The similarity with Fig. 1 with Ref. 18 is nonetheless evident.

What is usually referred to as the Kittel Law for domains[24] (1946) was actually discovered by Landau and Lifshitz[25] even earlier in 1935. Kittel[24] made the point that for thin films there are three basic kinds of rectilinear domains, illustrated in Fig. 4. For thick films ($d >$ 0.5 μm), the stable form has 180° antiparallel domains but with 45° facets so that no polarization is perpendicular to the outer surface (or electrode). This is case I in Fig. 4. For thickness $d < 0.5$ mm, the stable case is a single domain with polarization P (or magnetization M) in-plane (case III).

However, in small particles or (nanocubes or nanospheres), the stable state will be a circular domain composed of four 90° domains wound around a circle (Fig. 5). This has nothing to do with magnetoelectricity (although we will see later that magnetoelectrics might have circular or toroidal domains for an entirely different reason); it is simply the result of boundary conditions and surface effects in small particles.

These nanodomains are well known in magnetic materials, both natural and synthetic, and are best studied by electron holography. A beautiful illustration in ilmenite with nanoregions of Ti is shown in Fig. 6.[26] These "vortex domains" are best modeled[27] in terms of "winding numbers," as illustrated in Fig. 7.

For the flat films, the Landau–Lifshitz–Kittel model shows that surface energy and domain wall energy balance in such a way as to give a 180° stripe width w for domains with in-plane polarization (or magnetization) that depends upon the film thickness D

$$w^2/D = \text{constant} \quad . \tag{3}$$

Unfortunately, the constant is rather complicated to

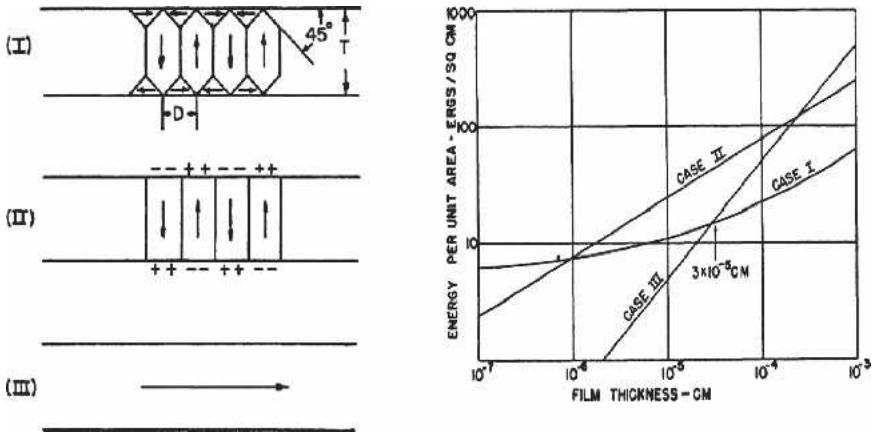

FIG. 4. Stable domain configurations in thin films as a function of film thickness.[24]

evaluate experimentally, and is very different (larger) for magnets than for ferroelectrics.

However, this equation can be scaled to be dimensionless, either by dividing both sides of Eq. (3) by the extrapolation length[28,29] or, which is much easier for experimentalists, the domain wall thickness T.[30] When this is done,[16] the result is

$$w^2/DT = [2\pi^3/21\ \zeta(3)]\ [\chi(\zeta)/\chi(x)]^{1/2} \quad , \qquad (4)$$

where $\zeta(3)$ is the Riemann zeta function of Eq. (3) and arises as an infinite sum of dipoles along a line of domains; $\chi(i)$ is the electric (or magnetic) susceptibility parallel or perpendicular to the polarization (magnetization).

This equation works extremely well (Fig. 8) for a wide range of ferroelectrics (Rochelle salt, lead titanate, and barium titanate) and magnets (Ni, Co, and LSMO). It also resolves some earlier controversies regarding ferroelectric domain wall widths; although many experimentalists have reported that these can be tens of nanometers wide, in reality the newer experimental work (Floquet and Valot[31,32]) and theory (Meyer and Vanderbilt[33]) indicate that they are one unit cell wide (~0.4 nm), with wider values arising from time-averaged excursions of the wall due to thermal motion.

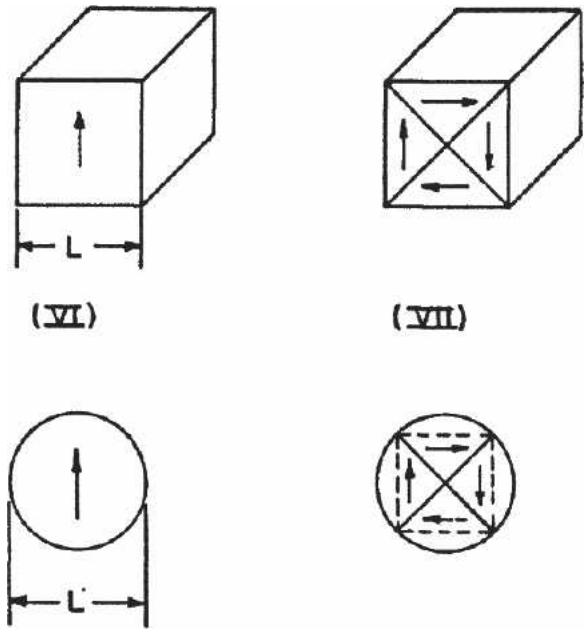

FIG. 5. Stable domain configurations in small particles (theory).[24]

E. Nanostructures

Although in principle nanoferroelectrics and multiferroics are two different topics, in reality they are apt to be combined in mostly commercial device embodiments. In particular, the development of a RAM in which the storage cell for each bit could be read magnetically (and nondestructively, with no reset required) but erased and rewritten electrically (faster, with lower power consumption) would combine the best qualities of both ferroelectric RAMs (FeRAMs) and magnetic memories. Therefore, it is useful to look at existing submicron ferroelectric memories to see where magnetoelectric RAMs might fit in.

Figure 9 illustrates the layout of the Samsung 4-Mb FeRAM. It consists of 512-kb blocks, each having 16 sections of 32 kb. This is a three-metal system with planar lead zirconate titanate (PZT) capacitors and Ir/IrO_2 and Pt/IrO_2 electrodes. Its scanning electron microscopy (SEM) cross section is shown in Fig. 10. A more advanced 32-Mb FeRAM is shown in cross section in Fig. 11. Note the tungsten plug and aluminum plate line. Figure 12 shows the latest 64-Mb FeRAM from Samsung. Note that the top electrode is now strontium ruthenate.

In the laboratory, we can go to much greater densities for prototype devices. Figure 13 shows a three-dimensional (3D) dynamic RAM (DRAM) trench with Ru electrodes from Kawano et al.[34]; Fig. 14 shows Ru lining a similar (3D) trench[35] prepared with our mist deposition system.

It would be useful to start filling such a 3D array with

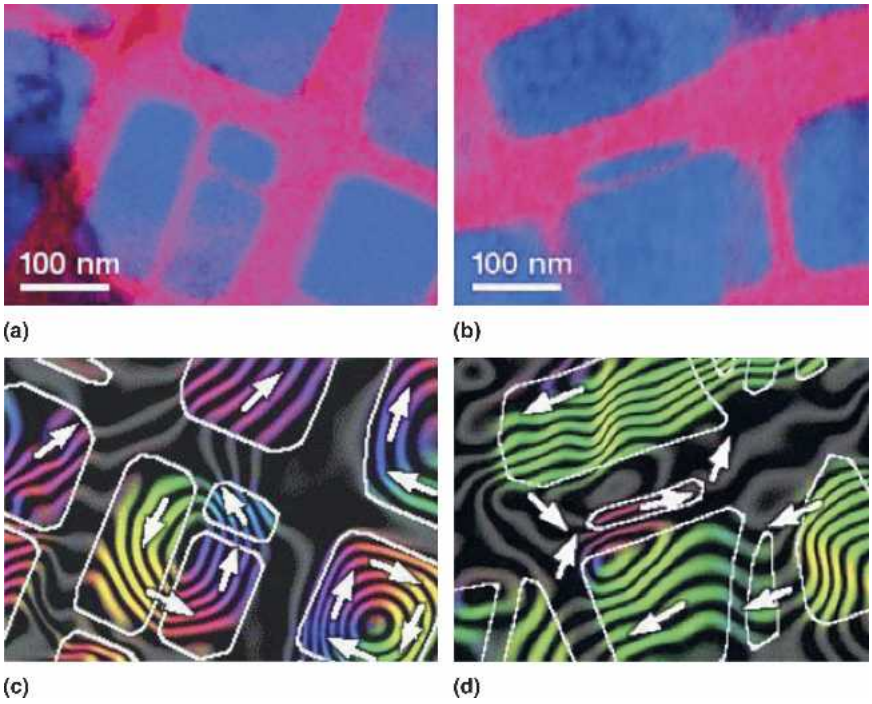

FIG. 6. Stable domain configurations in nanoparticles (experiment electron holography[26]).

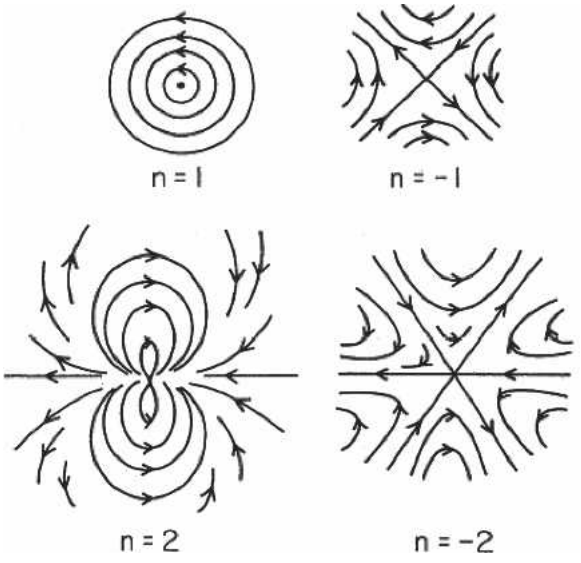

FIG. 7. Vortex structure of circular domains for different winding numbers (theory[27]).

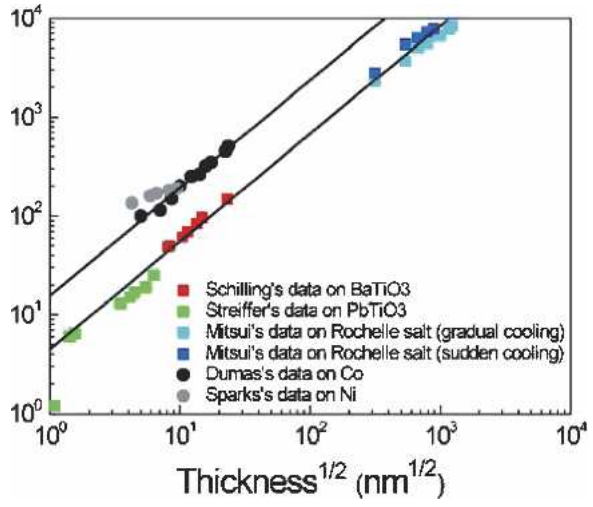

FIG. 8. Domain stripe width in ferroelectrics and ferromagnets versus the square root of film thickness; if this quantity is divided by the domain wall thickness, the two curves collapse to a single line given by Eq. (4)[23]; the solid lines shown are Eq. (4).

magnetoelectric materials, and a European Union-funded collaborative program is underway at Cambridge to do so. The state of the art for interconnect density is shown in Fig. 15, which is a cross-sectional view of porous Al_2O_3 filled with Pt to make interconnects onto barium titanate.[36] This gives an addressable array of nearly 1 Tb per square inch. The contact between the Pt and $BaTiO_3$ is atomically smooth, as shown by the transmission electron microscopy cross section in Fig. 16. And the resulting hysteresis for barium titanate or PZT (Fig. 17) is good. Note that an electrode interconnect area of 30 nm diameter is still sufficient to switch ~2000 electrons, enough for a sense amplifier to detect and read as a "1."

F. Ovidko–Gutkin theory

As we make nanowires, nanorods, and nanotubes from ferroelectrics and magnetoelectrics, it is useful to examine new theories relating to their performance. There are qualitative differences between epitaxial thin films in

https://doi.org/10.1557/jmr.2007.0260

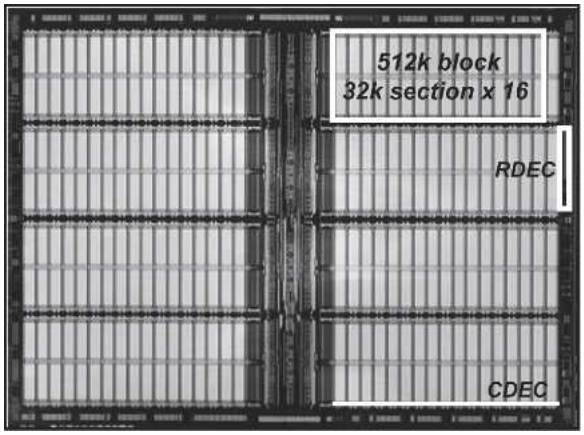

FIG. 9. Layout of Samsung 4 Mb PZT FeRAM (courtesy of D.J. Jung).

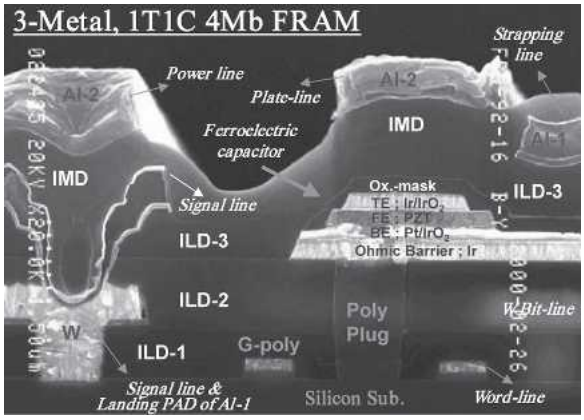

FIG. 10. SEM cross section of Samsung 4 Mb FeRAM (courtesy of D.J. Jung).

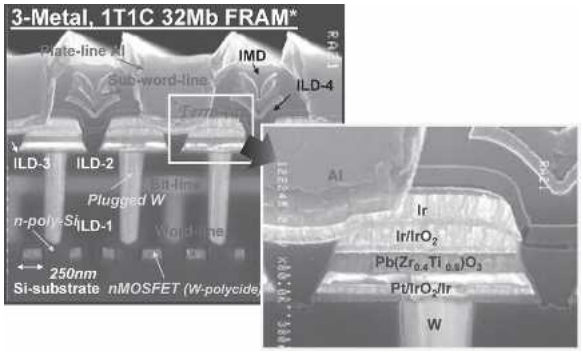

FIG. 11. SEM cross section of Samsung 32 Mb FeRAM (courtesy of D.J. Jung).

planar geometries and epitaxial thin films wrapped around to make nanotubes. Gutkin et al., [37] Scheinerman and Gutkin,[38] and Bobylev et al.[39] have developed a theory of misfit dislocations in the latter. They have found that for large-diameter nanotubes epitaxially grown on an inner core (or substrate), there are dense periodic misfits, as in planar epitaxial films. But in smaller-diameter nanotubes, these misfits become sparse and aperiodic. And in very narrow nanotubes, misfits are

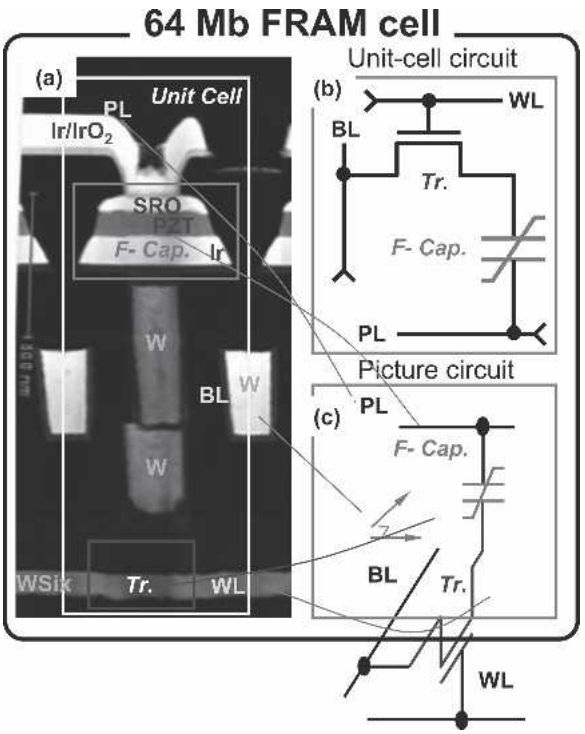

FIG. 12. (a) A micrograph of a cross-sectional view showing a unit-cell structure of 64-Mb of ferroelectric random access memory (FRAM), recently developed by Samsung (2006). (b) A standard textbook schematic circuit diagram of 1 bit memory of an FRAM with 1T1C cell configuration, consisting of both 1-transistor, one node of which is connected to a bit-line (BL) to transfer data by accessing word-line (WL), and 1-capacitor, one of which is connected to a plate-line (PL). (c) A schematic circuit diagram for the actual 64-Mb 1T1C memory with real geometry, corresponding to the micrograph in (a). Samsung Proprietary (courtesy of D.J. Jung). IMD, intermetal dielectric; inter-layer dielectric (ILD).

absent. The reason is that, unlike the case of epitaxial planar films, epitaxial nanotubes have cylindrical boundary conditions that cause misfit dislocations that cost energy.

It would be highly desirable to calculate phase diagrams for epitaxial nanotubes as functions of misfit parameter and temperature. At present, ab initio theories use similar periodic boundary conditions, but they cannot calculate the results for a sufficiently large number of atoms to correspond to even the thinnest nanotubes (experimentally about 10 nm in inner diameter, roughly 50 nm or 125 atoms in circumference).

It is also useful to remind ourselves that ferroelectric nanotubes experimentally have polarization along the tube (P_z), radially through the wall (P_r), and azimuthally around the wall (P_f). The azimuthal component is apparently large and is what is measured if one applies an antiferromagnetic tip to the top surface of a broken ferroelectric nanotube prone on the surface of a conducting substrate.[40] Unfortunately, although the exact calculations for piezo-response have been published[41–43] for P_z and P_r, the P_f model has not yet been done. Therefore, atomic

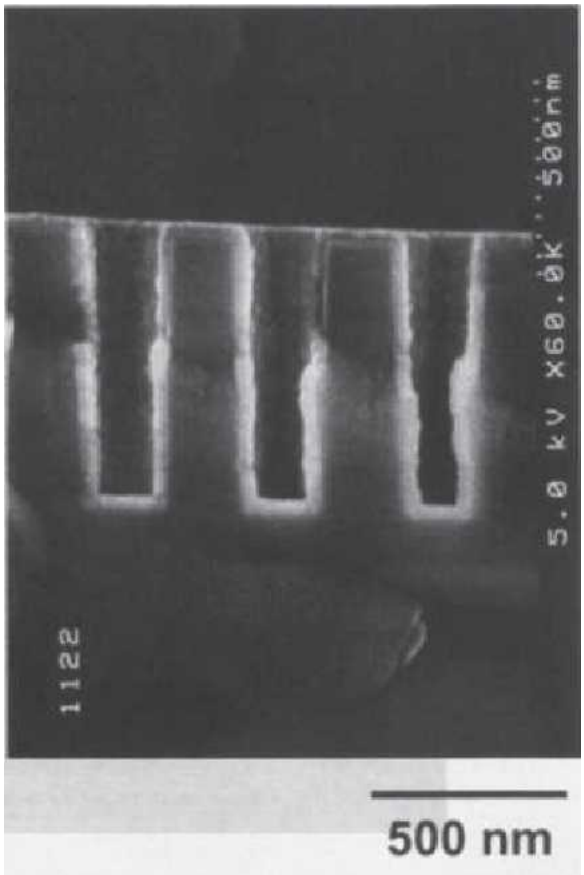

FIG. 13. Ru electrode deposited along the walls of a DRAM trench.[27]

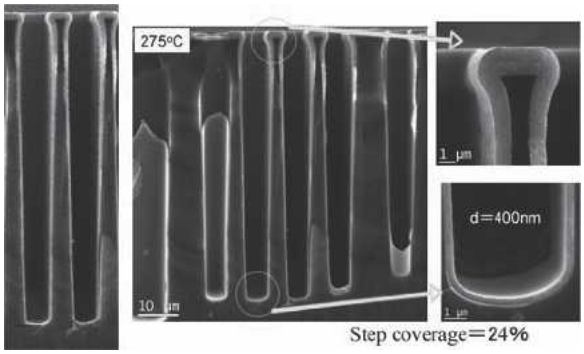

FIG. 14. PZT capacitor deposited along the sidewalls of a DRAM trench.[28]

force microscopy measurements cannot be directly related to the exact a_{ijk} piezoelectric coefficients of the materials. It is essential that these things be done before quantitative studies of magnetoelectric nanotubes can be carried out.

G. Fractal dimensionality

There is growing evidence[44–46] that the nucleation and growth of ferroelectric domains is fractal with effective dimension d between 2.4 and 2.6. Critical exponent sets

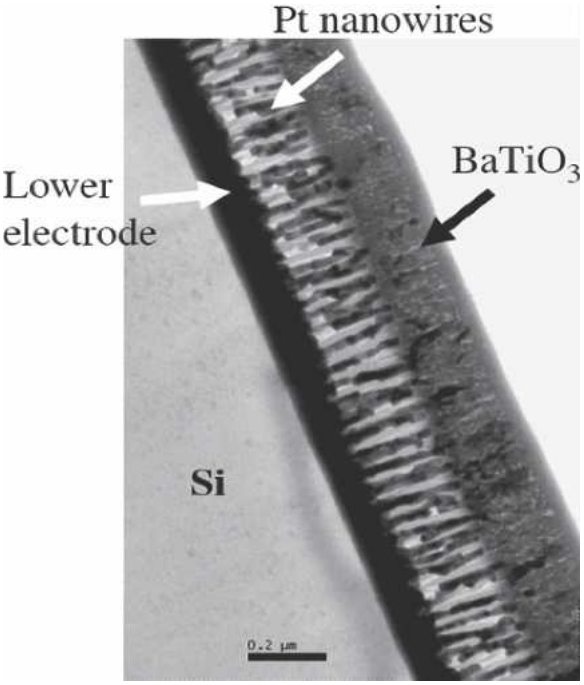

FIG. 15. Barium titanate (Tb per square inch) on Pt nanowire array. From Zhu et al.[29]

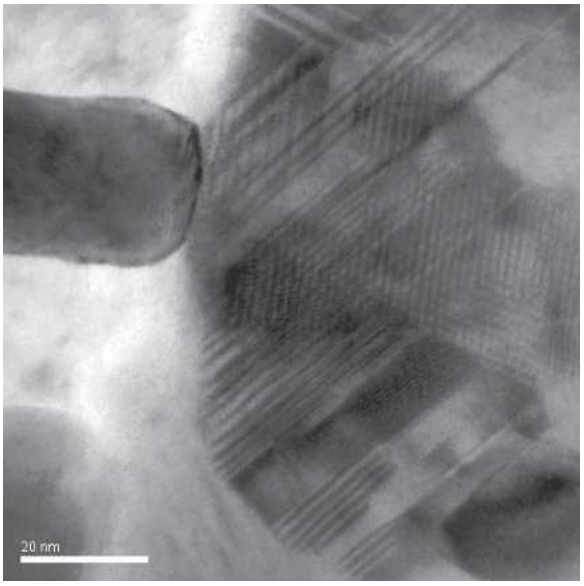

FIG. 16. Pt nanowire contact with $BaTiO_3$ capacitor, showing an atomically smooth interface.[29]

that are compatible with scaling and hyperscaling have also been published[47] for $d = 2.5$ and are shown in Table I. α, β, γ, and δ represent, in the usual notation, the exponents describing divergence of specific heat $C(T)$, polarization $P(T)$, dielectric constant e(T), and field dependence of polarization $P(E)$, respectively. Complicating the issue, however, is the possibility that defect dynamics, with different exponents, may dominate real materials.

https://doi.org/10.1557/jmr.2007.0260

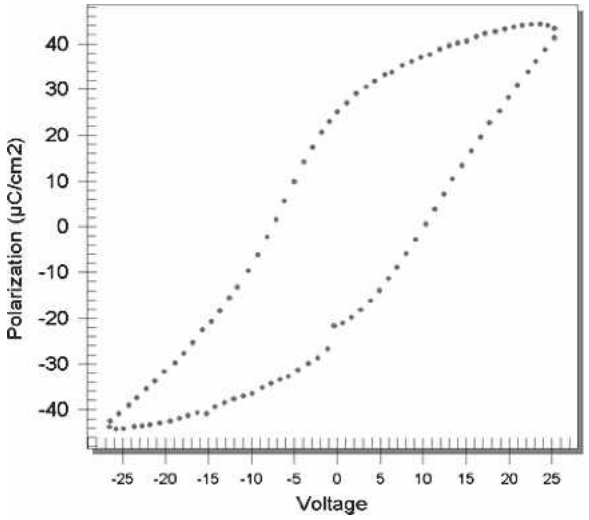

FIG. 17. Ferroelectric hysteresis for Pt–nanowire interconnects on PZT.[36]

TABLE I. Critical exponents in $d = 2.5$ dimensions (two possible sets satisfying scaling).

α	β	γ	δ
−½	¼	2	9
+⅓	⅓	1	4

Fractal dimensionality occurs in two other contexts for ferroelectrics and magnetoelectrics: The first is constant phase elements (CPEs), which occur in fitting dielectric data[48] that violate simple Cole–Cole plots or stretched exponentials. One microscopic model for the existence of CPEs is fractal geometries, where the self-similar structures give an infinite series of relaxation times. Another context is that of Curie–Von Schweidler polarization relaxation, in which the power-law decay of polarization current can be interpreted in terms of an infinite number of exponential decays superimposed in a self-similar fractal system.[49]

It would be useful to extend the study of fractal dimensionality to multiferroic materials.

H. Defect models

As mentioned above, there are reasons to believe that real ferroelectrics or magnetoelectrics will not exhibit true critical (fluctuation-dominated) dynamics near their T_C. Instead, the exponential dependencies of various thermodynamic properties, such as polarization, specific heat, and electric and magnetic susceptibilities, will be determined by defects. This was first discussed by Larkin and Khmelnitskii,[41] and then resurrected independently in 1979 by Levanyuk and Sigov[42] and by Imry and Wortis.[43] The defect "critical" effects were measured unambiguously later by several groups.[44,45] In magnetoelectric oxides, the primary defects are oxygen vacancies and corresponding multivalent states for the magnetic metal ions, such as Fe. Defect-critical exponents are nonasymptotic as T approaches T_C. Some are summarized in Table II.

In Table III, we see how the critical exponent b varies with dimension d for Ising-like systems, using the scaling formula below, where ν and η are the hyperscaling exponents describing correlation function $G(r,t)$ and the structure factor $S(q,t)$, respectively.

$$\beta(d) = \frac{\nu}{2}(d - 2 + \eta) \quad .$$

IV. TOROIDAL ORDERING IN MAGNETOELECTRICS

There has been a recent flurry of interest in the possibility of circular or toroidal domains [Figs. 18(a) and 18(b)] arising as a direct result of magnetoelectricity, and

TABLE II. Critical exponents in Levanyuk–Sigov defect theory.

α	β	γ	δ
½	0.4	½	2

TABLE III. Order parameter exponent β in Ising systems of dimension d.

$d = 2$	$d = 2.5$	$d = 3$	$d =$ infinity
⅛	¼	5/16	½

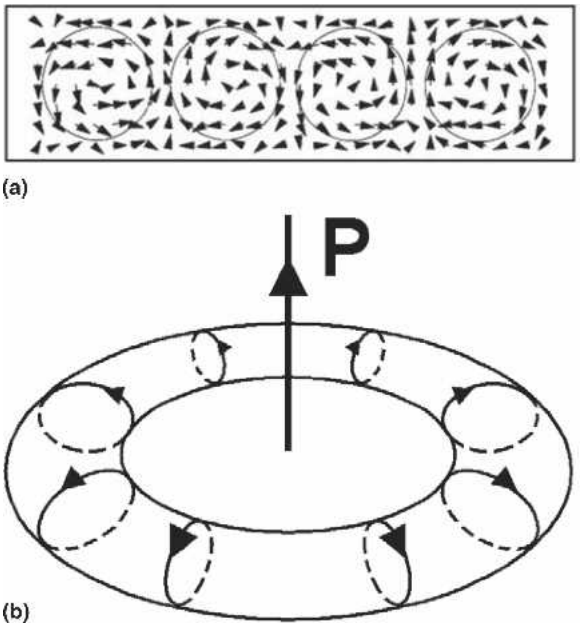

FIG. 18. (a) Toroidal ordering in ferroelectrics.[63] (b) Toroidal ordering in ferroelectrics.[56]

not, as discussed above, from very small particle sizes. This possibility was first developed theoretically by Ginzburg et al.[56] and Sannikov,[57,58] and was considered carefully by Dubovik and Tugushev[59] and Schmid.[60] Put on an ab initio basis, more recently,[61,62] it has been discussed widely[63,64] with application to RAMs suggested. The possibility of read-write operations is complex but facilitated via application of a direct current magnetic field.[65–67]

V. SUMMARY

I have presented some remarks on multiferroelectrics. Most of these new materials are being studied in the form of ceramic films. The fact that they are semiconducting presents problems for their electrical characterization and modeling. In addition, Maxwell–Wagner effects can produce extrinsic effects such as strong magnetocapacitance. Most of their device interest lies in nanostructures. For these, we have recently produced an extension of the Landau–Lifshitz–Kittel theory that is dimensionless (scaled in terms of the domain wall thickness or coherence length) that may facilitate treating domain walls in materials that are both magnetically and electrically ordered. Ab initio theories can deal with magnets and ferroelectrics, but it will be necessary in the future to extend them to include cylindrical boundary conditions for real nanotubes, finite temperatures, and fields, and probably semiconducting properties and nuisances like oxygen vacancy gradients. On the more academic side, there may be an interest in measuring critical phenomena; however, these may involve a fractal dimension of $d = 2.5$ and/or defect-dominated dynamics.

REFERENCES

1. G.A. Smolenskii: *Fiz. Tverd. Tela.* **1,** 149 (1959, in Russian).
2. B. Jaffe, W.R. Cook, and H. Jaffe: *Piezoelectric Ceramics* (Techbooks, New York [reprint issue], 1989).
3. W. Eerenstein, F.D. Morrison, J. Dho, M.G. Blamire, J.F. Scott, and N.D. Mathur: Comment on "Epitaxial $BiFeO_3$ multiferroic thin film heterostructures". *Science* **307,** 1203 (2005).
4. W. Eerenstein, F.D. Morrison, J.F. Scott, and N.D. Mathur: Growth of highly resistive $BiMnO_3$ films. *Appl. Phys. Lett.* **87,** 101906 (2005).
5. A. Perrier and A.J. Staring: *Arch. Sci. Phys. Nat. (Geneva)* **4,** 373 (1922).
6. A. Perrier and A.J. Staring: *Arch. Sci. Phys. Nat. (Geneva)* **5,** 333 (1923).
7. I.E. Dzyaloshinskii: *Zh. Eksp. Teor. Fiz.* **10,** 628 (1959, in Russian).
8. D.N. Astrov: *Zh. Eksp. Teor. Fiz.* **11,** 708 (1960, in Russian).
9. A.S. Borovik-Romanov: *Zh. Eksp. Teor. Fiz.* **11,** 786 (1960, in Russian).
10. S.L. Hou and N. Bloembergen: Paramagnetoelectric effects in $NiSO_4.6H_2O$ *Phys. Rev.* **138,** A1218 (1965).
11. J.F. Scott: Mechanisms of dielectric anomalies in $BaMnF_4$. *Phys. Rev.* **B16,** 2329 (1977).
12. A.M. Glass, M.E. Lines, M. Eibschutz, F.S.L. Hsu, and H.J. Guggenheim: Observation of anomalous pyroelectric behavior in $BaNiF_4$ due to cooperative magnetic singularity. *Commun. Phys.* **2,** 103 (1977).
13. G.A. Samara and J.F. Scott: Dielectric anomalies in $BaMnF_4$ at low-temperatures. *Solid State Commun.* **21,** 167 (1977).
14. J.F. Scott: Phase-transitions in $BaMnF_4$. *Rep. Prog. Phys.* **42,** 1055 (1979).
15. D.L. Fox and J.F. Scott: Ferroelectrically induced ferromagnetism. *J. Phys. C: Solid State Phys.* **10,** L329 (1977).
16. G. Catalan: Magnetocapacitance without magnetoelectric coupling. *Appl. Phys. Lett.* **88,** 102902 (2006).
17. T. Egami: Giant dielectric permittivity and magnetocapacitance in $La_{0.875}Sr_{0.125}MnO_3$ single crystals, in *Proceedings of the International Workshop on Fundamentals of Ferroelectricity* (Williamsburg, VA, March 2006).
18. D. Starešinić, P. Lunkenheimer, J. Hemberger, K. Biljaković, and A. Loidl: Giant dielectric response in the one-dimensional charge-ordered semiconductor $(NbSe_4)_3I$. *Phys. Rev. Lett.* **96,** 046402 (2006).
19. P. Lunkenheimer, R. Fichtl, J. Hemberger, V. Tsurkan, and A. Loidl: Relaxation dynamics and colossal magnetocapacitive effect in $CdCr_2S_4$. *Phys. Rev. B* **72,** 60103 (2005).
20. S. Weber, P. Lunkenheimer, R. Fichtl, J. Hemberger, V. Tsurkan, and A. Loidl: Colossal magnetocapacitance and colossal magnetoresistance in $HgCr_2S_4$. *Phys. Rev. Lett.* **96,** 157202 (2006).
21. J. Hemberger, P. Lunkenheimer, R. Fichtl, H-A. Krug von Nidda, V. Tsurkan, and A. Loidl: Multiferroic behavior in $CdCr_2X_4$ (X = S, Se). *Nature* **434,** 364 (2005).
22. C.J. Fennie and K.M. Rabe: Polar phonons and intrinsic dielectric response of the ferromagnetic insulating spinel CdCr2S4 from first principles. *Phys. Rev. B: Solid State* **72,** 214123 (2005); K.M. Rabe: (private communication, 2006).
23. G. Catalan and J.F. Scott: Comment on "Relaxor ferroelectricity and colossal magnetocapacitive coupling in ferromagnetic $CdCr_2S_4$" (arxiv/ cond-mat/0607500, 2006).
24. C. Kittel: Theory of the structure of ferromagnetic domains in films and small particles. *Phys. Rev.* **70,** 965 (1946).
25. L.D. Landau and E. Lifshitz: *Phys. Z. Sov. Union* **8,** 153 (1935, in Russian).
26. R.J. Harrison, R.E. Dunin-Borkowski, and A. Putnis: Direct imaging of nanoscale magnetic interactions in minerals. *Proc. Natl. Acad. Sci. U.S.A.* **99,** 16556 (2002).
27. N.D. Mermin: Topological theory of defects in ordered media. *Rev. Mod. Phys.* **51,** 591 (1979).
28. F. De Guerville, I.A. Luk'yanchuk, and L. Lahoche: Modeling of ferroelectric domains in thin films and superlattices. *Mater. Sci. Eng., B* **120,** 16 (2005).
29. V.A. Stephanovich, I.A. Luk'yanchuk, and M.G. Karkut: Domain-enhanced interlayer coupling in ferroelectric/paraelectric superlattices. *Phys. Rev. Lett.* **94,** 047601 (2005).
30. J.F. Scott: Nano-ferroelectrics: Statics and dynamics. *J. Phys.: Condens. Matter* **18,** R361 (2006).
31. N. Floquet and C. Valot: Ferroelectric domain walls in $BaTiO_3$: Structural wall model interpreting fingerprints in XRPD diagrams. *Ferroelectrics* **234,** 107 (1999).
32. N. Floquet, C.M. Valot, and M.T. Mesnier: Ferroelectric domain walls in $BaTiO_3$: Fingerprints in XRPD diagrams and quantitative HRTEM image analysis. *J. Phys. III (Paris)* **7,** 1105 (1997).
33. B. Meyer and D. Vanderbilt: Ab initio study of ferroelectric domain walls in $PbTiO_3$. *Phys. Rev. B* **65,** 104111 (2002).
34. K. Kawano, H. Kosuge, N. Oshima, and H. Funakubo: Conformability of ruthenium dioxide films prepared on substrates with capacitor holes by MOCVD and modification by annealing. *Electrochem. Solid-State Lett.* **9,** C175 (2006).
35. M. Miyake, F.D. Morrison, J.F. Scott, T. Tatsuta, and O. Tsuji:

Coating of DRAM trenches with Ru electrodes and PZT dielectric films via misted deposition. *Integ. Ferroelectrics.* (2007, in press).
36. X.H. Zhu, P.R. Evans, D. Byrne, A. Schilling, C. Douglas, R.J. Pollard, R.M. Bowman, J.M. Gregg, F.D. Morrison, and J.F. Scott: Perovskite lead zirconium titanate nanorings: Towards nanoscale ferroelectric "solenoids"? *Appl. Phys. Lett.* **89,** 129913 (2006).
37. M.Y. Gutkin, I.A. Ovid'ko, and A.G. Sheinerman: Misfit dislocations in wire composite solids. *J. Phys.: Condens. Matter* **12,** 5391 (2000).
38. A.G. Sheinerman and M.Y. Gutkin: Misfit disclinations and dislocation walls in a two-phase cylindrical composite. *Phys. Status Solidi A* **184,** 485 (2001).
39. S.V. Bobylev, M.Y. Gutkin, and I.A. Ovid'ko: Nanograins with 90 degrees grain boundaries in high transition temperature superconducting films. *J. Phys.: Condens. Matter* **15,** 7925 (2003).
40. Y. Luo, I. Szafraniak, V. Nagarajan, R.B. Wehrspohn, M. Steinhart, J.H. Wendorff, N.D. Zakharov, R. Ramesh, and M. Alexe: Ferroelectric lead zirconate titanate and barium titanate nanotubes Integ. *Ferroelectrics* **59,** 1513 (2003).
41. R. Ramesh and D.D. Ebenezer: Analysis of axially polarized piezoelectric ceramic rings. *Ferroelectrics* **323,** 17 (2005).
42. R. Ramesh and D.D. Ebenezer: Exact analysis of axially polarized piezoelectric ceramic cylinders with certain uniform boundary conditions. *Curr. Sci.* **85,** 1173 (2003).
43. R. Ramesh and D.D. Ebenezer: Analysis of axially polarized piezoelectric cylinders with arbitrary boundary conditions on flat surfaces. *J. Acoust. Soc. Am.* **113,** 1900 (2003).
44. P. Paruch, T. Giamarchi, and J-M. Triscone: Domain wall roughness in epitaxial ferroelectric $PbZr_{0.2}Ti_{0.8}O_3$ thin films. *Phys. Rev. Lett.* **94,** 197601 (2004).
45. S.V. Kalinin: (private communication, 2006).
46. W. Kleemann, J. Dec, S.A. Prosandeev, T. Braun, and P.A. Thomas: Universal domain wall dynamics in ferroelectrics and relaxors. *Ferroelectrics* **334,** 3 (2006).
47. J.F. Scott: Absence of true critical exponents in relaxor ferroelectrics: The case for defect dynamics. *J. Phys.: Condens. Matter* **18,** 7123 (2006).
48. J.R. Macdonald: *Impedance Spectroscopy* (Wiley, New York, 1987).
49. P. Curie: *Ann. Chim. Phys.* 18**,** 203 (1889); E. von Schweidler. *Ann. Phys.* **24,** 711 (1907).
50. A.I. Larkin and D.E. Khmelnitskii: *Zh. Eksp. Teor. Fiz.* **56,** 2087 (1969, in Russian).
51. A.P. Levanyuk and A.S. Sigov: *Izv. Akad. Nauk SSSR Ser. Fiz.* **43,** 1562 (1979, in Russian).
52. Y. Imry and M. Wortis: Influence of quenched impurities on 1st-order phase transitions. *Phys. Rev., B* **19,** 3580 (1979).
53. T.W. Ryan, R.J. Nelmes, R.A. Cowley, and A. Gibaud: Observation of two length scales for the critical fluctuations of $RbCaF_3$. *Phys. Rev. Lett.* **56,** 2704 (1986).
54. Y.M. Kishinetz, A.P. Levanyuk, A.I. Morosov, and A.S. Sigov: Dislocation- induced anomalies of physical properties of crystals near structural phase transitions. *Ferroelectrics* **79,** 321 (1988).
55. A.I. Murosov and A.S. Sigov: Influence of defects on phase transitions. *Comments Condens. Matt. Phys.* **18,** 279 (1998).
56. V.L. Ginzburg, A.A. Gorbatsevich, Y.V. Kopaev, et al., On the problem of superdiamagnetism. *Solid State Commun.* **50,** 339 (1984).
57. D.G. Sannikov: A sequence of two ferrotoroidal phase transitions in nickel-bromine boracite $Ni_3B_7O_{13}Br$. *JETP Lett.* **73,** 401 (2001); Dynamics of domain wall in ferrotoroic phase of boracites. *Ferroelectrics* **291,** 163 (2003).
58. D.G. Sannikov and I.S. Zheludev: Possibility of phase transition with spontaneous toroidal moment formation in nickel boracites. *Sov. Phys. Solid State* **27,** 826 (1985).
59. V.M. Dubovik and V.V. Tugushev: Toroid moments in electrodynamics and solid- state physics. *Phys. Rep.* **187,** 145 (1990).
60. H. Schmid: On ferrotoroids and electrotoroidic, magnetotoroidic and piezotoroidic Effects. *Ferroelectrics* **252,** 41 (2001).
61. M. Fiebig: Revival of the magnetoelectric effect. *J. Phys. D: Appl. Phys.* **38,** R123 (2005).
62. W. Eerenstein, N.D. Mathur, and J.F. Scott: Multiferroic and magnetoelectric materials. *Nature* **442,** 759 (2006).
63. I. Naumov, L. Bellaiche, and H. Fu: Unusual phase transitions in ferroelectric nanodisks and nanorods. *Nature* **432,** 737 (2004).
64. J.F. Scott: Ferroelectrics: Novel geometric ordering of ferroelectricity. *Nat. Mater.* **4,** 13 (2005).
65. I. Ponomarevna, I. Naumov, and L. Bellaiche: Low-dimensional ferroelectrics under different electrical and mechanical boundary conditions: Atomistic simulations. *Phys. Rev. B* **72,** 214118 (2005).
66. I. Ponomareva, I. Naumov, I. Kornev, H. Fu, and L. Bellaiche: Atomistic treatment of depolarizing energy and field in ferroelectric nanostructures. *Phys. Rev. B* **72,** 140102 (2005).
67. S. Prosandeev, I. Ponomareva, I. Kornev, I. Naumov, and L. Bellaiche: Controlling toroidal moment by means of an inhomogeneous static field: An ab initio study. *Phys. Rev. Lett.* **96,** 237601 (2006).